

Effects of Mg^{2+} on the Pre-Steady-State Kinetics of the Biotin Carboxylation Reaction of Pyruvate Carboxylase[†]

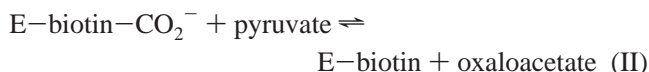
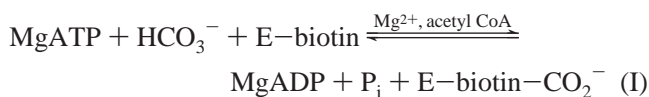
Joy P. Branson and Paul V. Attwood*

Department of Biochemistry, The University of Western Australia, Nedlands, WA 6907, Australia

Received December 9, 1999; Revised Manuscript Received April 10, 2000

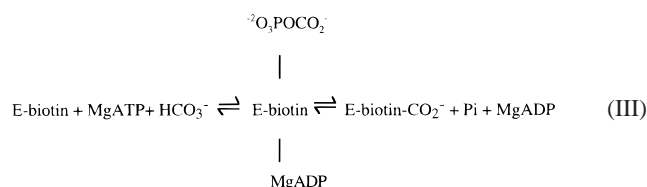
ABSTRACT: The effects of Mg^{2+} concentration on the kinetics of both ATP cleavage and carboxyenzyme formation in the approach to steady state of the biotin carboxylation reaction of pyruvate carboxylase have been studied. It was found that the enzyme underwent dilution inactivation at low Mg^{2+} concentrations and that this occurred at higher enzyme concentrations than had been previously observed. At 10 mM Mg^{2+} , dilution inactivation was prevented and activation of the enzyme also occurred. When the enzyme was mixed with an ATP solution to initiate the carboxylation reaction, dilution inactivation was reversed and further enzyme activation was induced to a final level that was dependent on Mg^{2+} concentration. With the exception of the reaction at 10 mM Mg^{2+} in the presence of acetyl CoA, the experimental data could be adequately described as first-order exponential approaches to steady state. At 10 mM Mg^{2+} in the presence of acetyl CoA, both ATP cleavage and carboxyenzyme formation data were best described as a biexponential process, in which there was little ATP turnover at steady state. Modeling studies have been performed which produced simulated data that were similar to the experimental data, using a reaction scheme modified from one proposed previously [Legge, G. B., et al. (1996) *Biochemistry* 35, 3849–3856]. These studies indicate that the major foci of action of Mg^{2+} are in the decarboxylation of the enzyme–carboxybiotin complex, the return of the biotin to the site of the biotin carboxylation reaction, and the coupling of ATP cleavage to biotin carboxylation.

Pyruvate carboxylase (EC 6.4.1.1) is a biotin-dependent enzyme that catalyzes the carboxylation of pyruvate to form oxaloacetate, and the overall reaction that it catalyzes proceeds in two steps as follows:



The first partial reaction of pyruvate carboxylase (reaction I) requires carboxylation of the biotin prosthetic group by HCO_3^- with concomitant cleavage of MgATP. The second partial reaction (reaction II) involves the carboxylation of pyruvate by carboxybiotin. Free Mg^{2+} and acetyl CoA are only required in reaction I, but the degree of dependence on acetyl CoA for activity depends on the source of the enzyme (for a review, see ref 1). In the work presented here, chicken liver pyruvate carboxylase was used and this exhibits almost complete dependence on acetyl CoA for activity. Mg^{2+} is known to be required in the biotin carboxylation reaction, although its exact role in this reaction is not well understood.

Current available evidence suggests that reaction I proceeds via a carboxyphosphate intermediate as shown in reaction III (see ref 2 for a review).



Scrutton et al. (3) showed that incubation of pyruvate carboxylase with Mg^{2+} , MgATP, $\text{H}^{14}\text{CO}_3^-$, and acetyl CoA resulted in the formation of a [^{14}C]carboxyenzyme complex. Phillips et al. (4) investigated the reaction presented above and suggested that in the absence of acetyl CoA, the [^{14}C]carboxyenzyme complex formed was in fact the enzyme–[^{14}C]carboxyphosphate complex, which on addition of acetyl CoA resulted in the transfer of the [^{14}C]carboxy group to biotin to form the enzyme–[^{14}C]carboxybiotin complex. However, Attwood (5) showed that the [^{14}C]carboxyenzyme complex formed in the absence of acetyl CoA behaved in the same way as the enzyme–[^{14}C]carboxybiotin complex in its ability to carboxylate pyruvate in the absence of any other substrates or effectors. Hence, it seems incubation of the enzyme with Mg^{2+} , MgATP, and HCO_3^- results in the steady-state formation of a carboxyenzyme complex that is in fact the enzyme–carboxybiotin complex.

Attwood and Graneri (6) showed that pyruvate carboxylase was capable of catalyzing the release of phosphate from

[†] This work was supported by grants (04/15/412/237 and A09943118) from the Australian Research Council to P.V.A.

* To whom correspondence should be addressed: Department of Biochemistry, The University of Western Australia, Nedlands, WA 6907, Australia. Phone: 61 8 9380 3329. Fax: 61 8 9380 1148. E-mail: pattwood@cylle.uwa.edu.au.

MgATP in the presence of HCO_3^- and Mg^{2+} in the absence of pyruvate and in the presence or absence of acetyl CoA. However, these steady-state reactions proceeded at less than 0.1% of the rate of the full pyruvate carboxylation reaction, and the authors suggested that the rate-limiting step in the catalytic cycle in the absence of pyruvate was the decarboxylation of the carboxyenzyme complex. Legge et al. (7) showed that acetyl CoA increased the rate constants for the approach to steady state and greatly enhanced the degree of coupling of ATP cleavage to carboxybiotin formation. In the absence of acetyl CoA, the decarboxylation of carboxyphosphate is rapid relative to carboxybiotin formation. The authors suggested that the major effect of acetyl CoA was to enhance the rate of the step in which the putative carboxyphosphate is formed and enhance the degree of coupling the formation of the enzyme-carboxybiotin complex to ATP cleavage.

To further understand how Mg^{2+} is involved in the biotin-carboxylation reaction of chicken liver pyruvate carboxylase, the effects of Mg^{2+} concentration on the kinetics of ATP cleavage and carboxyenzyme formation in the presence and absence of acetyl CoA were investigated. Using a combination of pre-steady-state kinetic measurements and kinetic modeling, a reaction scheme is proposed which helps to further elucidate the roles of acetyl CoA and Mg^{2+} in the biotin carboxylation reaction.

EXPERIMENTAL PROCEDURES

Preparation of Chicken Liver Pyruvate Carboxylase. Chicken liver pyruvate carboxylase was purified as described by Goss et al. (8), except that a DEAE-Sephacel CL-6B column was used in place of the DEAE-Sephadex column. The enzyme was purified to an average specific activity of 20–30 units/mg of protein (1 unit of enzyme activity is defined as the amount of protein required to catalyze the formation of 1 μmol of oxaloacetate/min with saturating substrate concentrations, at 30 °C). The enzyme was stored at –80 °C in a storage solution containing 0.1 M Tris-HCl (pH 7.2), 1.6 M sucrose, and 40 mM $(\text{NH}_4)_2\text{SO}_4$. Prior to the experiments, the enzyme was transferred from the storage solution to 0.1 M Tris-HCl (pH 7.8) by centrifugation through Sephadex G-25 as described by Helmerhorst and Stokes (9). The purities of the enzyme preparations were estimated to be between 75 and 88% by SDS-gel capillary electrophoresis.

Other Materials. From Amersham Australia Pty. Ltd., $\text{NaH}^{14}\text{CO}_3$ was obtained as an aqueous solution at a specific radioactivity of 55 mCi/mmol and $[^{14}\text{C}]$ biotin was obtained as a solid at a specific radioactivity of 50–62 mCi/mmol. $[\gamma\text{-}^{32}\text{P}]\text{ATP}$ was obtained as an aqueous solution of the triethylammonium salt at a specific radioactivity of approximately 3000 Ci/mmol from Du Pont NEN. All other materials were highly pure preparations from commercial suppliers.

Spectrophotometric Pyruvate Carboxylase Assays. The conditions for this assay were described by Attwood and Cleland (10), except that the buffer that was used was 0.1 M Tris-HCl (pH 7.8). After transfer of the enzyme from storage buffer to 0.1 M Tris-HCl (pH 7.8), assays were performed in triplicate at 30 °C. For the determination of the turnover number of the enzyme, the assays were performed as described above except the temperature was 20 °C and the concentration of HCO_3^- was 15 mM, as in the quenched-flow experiments.

Biotin Determination. After removal from storage solution, aliquots of the enzyme solutions were set aside and stored at –80 °C for later determination of the biotin content. The enzyme solutions were incubated with 0.2% (w/v) chymotrypsin at 37 °C for 24 h. Pronase was then added to a final concentration of 0.45% (w/v), and the solutions were incubated for an additional 72 h at 37 °C. The solutions were then heated for 15 min at 100 °C before being used in the biotin assay described by Rylatt et al. (11).

Changes in Enzyme Specific Activity That Occur during the Reaction. In the experiments designed to assess ATP cleavage and carboxyenzyme formation in the absence of acetyl CoA, a solution of the enzyme (70 units/mL) was prepared by diluting a stock solution of enzyme (300–400 units/mL) into 0.1 M Tris-HCl (pH 7.8) containing either 0.1, 1.0, or 10 mM MgCl_2 and 15 mM NaHCO_3 . The reactions were initiated by mixing this enzyme solution with an equal volume of a similar solution that contained either 5.1, 6.0, or 15 mM MgCl_2 , 15 mM NaHCO_3 , and 5 mM ATP, but no enzyme. Both the enzyme and ATP solutions were incubated at 20 °C for 10 min prior to mixing. Changes in total enzyme activity that occurred after this mixing process were monitored by withdrawing aliquots at various times from the reaction mixture and assaying them for pyruvate carboxylating activity using the spectrophotometric assay described above.

ATP Cleavage Experiments at Various Concentrations of Free Mg^{2+} in the Presence or Absence of Acetyl CoA. The effects of different Mg^{2+} concentrations on the kinetics of ATP cleavage were determined as described by Legge et al. (7). Briefly, enzyme and ATP reaction solutions were prepared; the enzyme solutions contained all reaction components, except ATP, while the ATP solutions contained all reaction components, except enzyme. These reaction solutions were preincubated at 20 °C for least 10 min before the reactions were initiated by mixing equal volumes of the enzyme and ATP solutions. The concentration of ATP in the reaction itself was 2.5 mM, with approximately 30 $\mu\text{Ci}/\mu\text{mol}$ of $[\gamma\text{-}^{32}\text{P}]\text{ATP}$, and the concentrations of MgCl_2 were 2.6, 3.5, and 12.5 mM, giving a free Mg^{2+} concentration of 0.24, 1.0, or 10.0 mM. The free Mg^{2+} concentration was calculated using the MgATP dissociation constant of 0.0143 mM (12). The final reaction concentration of enzyme was 35 units/mL (17.2–19.6 μM biotin) in the reactions in the absence of acetyl CoA and 105 units/mL (40.7–67.4 μM biotin) in its presence. Reactions were performed in 0.1 M Tris-HCl (pH 7.8) at 20 °C in the presence of 15 mM NaHCO_3 . Reactions were stopped at various times by addition of 1.25 volumes of 2 M HCl. The enzyme was precipitated from the solution by addition of ice-cold trichloroacetic acid, and the amount of $[\gamma\text{-}^{32}\text{P}]\text{P}_i$ released from $[\gamma\text{-}^{32}\text{P}]\text{ATP}$ was measured as described previously (7). Reactions carried out in the presence of acetyl CoA were performed on a Hi-Tech PQ/SF 53 preparative quench/stopped-flow spectrophotometer, while those in its absence were performed manually.

Carboxyenzyme Formation Experiments at Various Concentrations of Free Mg^{2+} in the Absence or Presence of Acetyl CoA. The effects of different Mg^{2+} concentrations on the kinetics of carboxyenzyme formation were determined as described by Legge et al. (7), except the free Mg^{2+} concentration was 0.24, 1.0, or 10.0 mM, as described above.

for the ATP cleavage experiments. Briefly, enzyme and ATP reaction solutions were prepared and the reactions initiated by mixing equal volumes of these solutions as described above for the ATP cleavage experiments. In this case, however, no $[\gamma\text{-}^{32}\text{P}]\text{ATP}$ was present and the 15 mM NaHCO_3 was replaced with 12.5 mM NaHCO_3 and 2.5 mM $\text{NaH}^{14}\text{CO}_3$. Reactions were stopped at various times after mixing by addition of an equal volume of a quench solution containing 200 mM pyruvate, 0.4 mM NADH, 22 units/mL malate dehydrogenase, 200 mM ethylenediaminetetraacetic acid (EDTA), and 400 mM NaHCO_3 adjusted to pH 7.8. As described previously (7), the EDTA forms complexes with Mg^{2+} in the reaction mixtures, thus stopping the reaction, and the large excess of NaHCO_3 dilutes out the $\text{NaH}^{14}\text{CO}_3$, reducing the possibility of further incorporation of $^{14}\text{CO}_2^-$ into carboxyenzyme. The ^{14}C carboxyenzyme reacts with pyruvate to form ^{14}C oxaloacetate which is then converted to more stable ^{14}C malate in a reaction catalyzed by the malate dehydrogenase. The solutions were then acidified to remove $\text{NaH}^{14}\text{CO}_3$, and the amount of radioactivity incorporated into ^{14}C malate was measured, which is equivalent to the radioactivity that was incorporated into ^{14}C carboxyenzyme, essentially in the form of ^{14}C carboxybiotin, when the reaction was stopped (7). The concentration of enzyme in the reaction solutions was 35 units/mL (13.8–19.6 μM biotin).

Data Analysis. The kinetic data were analyzed using nonlinear least-squares regression analysis to fit one of the following equations to the data described in detail in the text:

$$y = A(1 - e^{-kt}) \quad (1)$$

$$y = A(1 - e^{-kt}) + rt \quad (2)$$

$$y = A(1 - e^{-kt}) + B \quad (3)$$

$$y = A(1 - e^{-kt}) + A'(1 - e^{-k't}) \quad (4)$$

$$y = k_1 C_A (e^{-k_1 t} - e^{-k_2 t}) / (k_2 - k_1) \quad (5)$$

where y is either the number of moles of carboxyenzyme formed per mole of biotin or the number of moles of P_i released per mole of biotin, A and A' are the amplitudes of the approach to steady state, r is the steady-state turnover number, and B is any residual at time zero. In eq 5, C_A is the initial proportion of enzyme that reacts to form carboxyenzyme; k_1 is the rate constant for the formation of carboxyenzyme, while k_2 is the rate constant for its removal. Simulations of kinetic models were performed by a numerical integration method similar to that described by Legge et al. (7).

RESULTS

Figure 1 shows the changes in specific enzyme activity that occurred when the enzyme solution was mixed with the ATP solution at the three different Mg^{2+} concentrations in the absence of acetyl CoA. The zero time points were calculated from assays of the enzyme solution prior to mixing with the ATP solution. As calculated from the stock enzyme solution, all of the zero time point enzyme specific activities should have been 20 units/mg; however, at both 0.24 and 1.0 mM Mg^{2+} , these enzyme specific activities were 13.1 and 17.1 units/mg, respectively, while at 10 mM Mg^{2+} , the zero time specific activity was 24.5 units/mg. Following

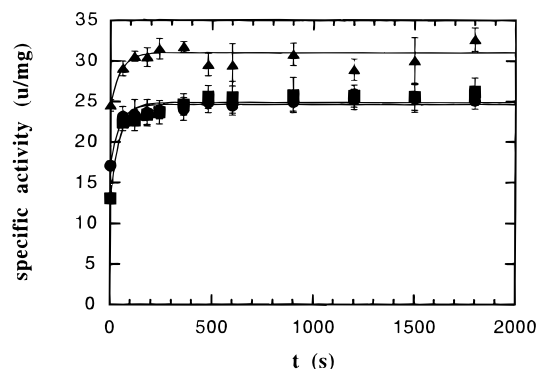


FIGURE 1: Changes in the specific activity of pyruvate carboxylase were determined under the conditions used to measure the kinetics of the biotin carboxylation reactions in the absence of acetyl CoA, i.e., at 20 °C in a solution of 0.1 M Tris-HCl (pH 7.8) containing 15 mM NaHCO_3 and 2.5 mM ATP and with 0.24 (■), 1.0 (●), or 10 mM free Mg^{2+} (▲), as described in Experimental Procedures. Specific activity was measured by removal of aliquots of the reaction mixture containing the enzyme and assaying for pyruvate carboxylating activity by spectrophotometric assay in which the oxaloacetate formed is converted to malate by malate dehydrogenase with concomitant oxidation of NADH. Times refer to the time after mixing equal volumes of enzyme solution and ATP solution. The lines represent nonlinear least-squares fits to the data of eq 3. The data points represent the means and the error bars the standard deviations from the mean of three determinations.

mixing, the enzyme specific activity rose rapidly at all Mg^{2+} concentrations such that the final activities that were achieved were approximately 24.7, 24.6, and 31.0 units/mg, at 0.24, 1.0, and 10 mM, respectively. At the time of the first assay after mixing (1 min), the enzyme specific activities had risen by 79, 74, and 72% of the total increases in enzyme specific activity at 0.24, 1.0, and 10 mM Mg^{2+} , respectively. Fits of single-exponential curves (eq 3) to the data are shown in Figure 1 and give apparent first-order rate constants of about 0.02 s^{-1} in all cases. However, because of the rapid nature of the increase in activity relative to the spacing of the measurements, the single-exponential nature of the processes and the values of the rate constants that are obtained cannot be regarded as definitive.

In similar experiments where both the enzyme and ATP solutions contained acetyl CoA, no dilution inactivation was observed and the enzyme specific activities did not increase up to 1 min after mixing the solutions together.

Figure 2 shows the approach to steady state of the ATP cleavage reaction (A) and the formation of the carboxyenzyme complex (B) at the three different Mg^{2+} concentrations in the absence of acetyl CoA. Nonlinear least-squares fits of eq 2 to the ATP cleavage data were obtained, indicating a first-order approach to steady state, and the kinetic parameters obtained from these fits are shown in Table 1. The amplitudes of the burst phase in the approach to steady state for ATP cleavage appear to increase with increasing Mg^{2+} concentrations. The standard errors on the estimates of the apparent first-order rate constants for the approach to steady state overlap, and this would suggest that there is little dependence of this parameter on Mg^{2+} concentration. The steady-state turnover number initially increased in going from 0.24 to 1 mM Mg^{2+} by a factor of 2.7; however, when the Mg^{2+} concentration increased to 10 mM, the turnover number was reduced to 57% of that at 1 mM Mg^{2+} .

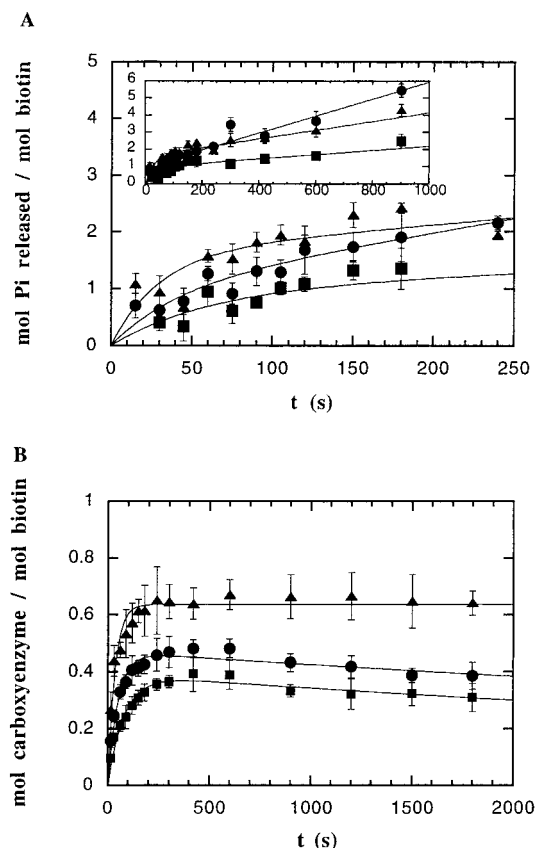


FIGURE 2: Kinetics of ATP cleavage (A) and carboxyenzyme formation (B) measured at 20 °C in 0.1 M Tris-HCl (pH 7.8) in the presence of 0.24 (■), 1.0 (●), and 10 mM Mg²⁺ (▲), as described in Experimental Procedures. For panel A, 2.5 mM [γ -³²P]-ATP and 15 mM NaHCO₃ were present, while for panel B, 2.5 mM ATP, 12.5 mM NaHCO₃, and 2.5 mM NaH¹⁴CO₃ were present. In panel A, the amount of P_i released per mole of biotin corresponds to the total number of moles of ATP cleaved per mole of biotin, and the data have been corrected for HCO₃⁻-independent ATP cleavage as described in Experimental Procedures. The lines represent nonlinear least-squares fits of eq 2 to the data. The main panel shows the first 250 s of the reaction time course, while the inset shows the full time course. In panel B, the number of moles of carboxyenzyme formed per mole of biotin corresponds to the total amount of carboxyl groups that can be transferred to pyruvate on quenching. The lines represent nonlinear least-squares fits of eq 1 to the 10 mM Mg²⁺ data and of eq 5 to the 0.24 and 1 mM Mg²⁺ data. The data points in panels A and B represent the mean and the error bars the standard deviation of three separate measurements from three separate time course experiments.

Table 1: Kinetic Parameters Derived from Fits of Eq 2 to ATP Cleavage Data in the Absence of Acetyl CoA and Data Simulated from Scheme 1

	k (s ⁻¹)	A (mol of P _i /mol of biotin)	r (turnover no.) (s ⁻¹)
experimental data			
0.24 mM Mg ²⁺	0.018 ± 0.009	0.92 ± 0.20	0.0018 ± 0.0004
1 mM Mg ²⁺	0.014 ± 0.008	1.29 ± 0.36	0.0049 ± 0.0006
10 mM Mg ²⁺	0.025 ± 0.009	1.66 ± 0.20	0.0028 ± 0.0004
simulated data			
0.24 mM Mg ²⁺	0.012 ± 0.001	0.81 ± 0.04	0.0021 ± 0.00003
1 mM Mg ²⁺	0.016 ± 0.001	1.60 ± 0.03	0.0047 ± 0.00003
10 mM Mg ²⁺	0.025 ± 0.0002	1.56 ± 0.004	0.0030 ± 0.000004

The kinetics of carboxyenzyme formation shown in Figure 2B are complex and do not correspond to simple first-order approaches to a steady-state level, except perhaps at 10 mM Mg²⁺ where a nonlinear least-squares fit of eq 1 was

obtained. At 0.24 and 1 mM Mg²⁺, the kinetics indicate that there is an initial rapid formation of carboxyenzyme followed by a slower reaction in which it is removed, and such a process is described by eq 5. As can be seen from Figure 2B, good fits of eq 5 to the data at 0.24 and 1 mM Mg²⁺ were obtained. The amplitude of the initial increase in the level of carboxyenzyme and the rate constant for this phase of the reaction were dependent on Mg²⁺ concentration. The greater the Mg²⁺ concentration, the larger the amplitude of the initial increase and the larger the rate constant, and there is little difference between the rate constants of the slower, decay phase at 0.24 and 1 mM Mg²⁺ (see Table 2).

Figure 3 shows the kinetics of the approach to steady state of the ATP cleavage reaction (A) and the formation of the carboxyenzyme complex (B) at three different Mg²⁺ concentrations in the presence of acetyl CoA. Adequate fits of eq 2 were obtained to the ATP cleavage data at 0.24 and 1.0 mM Mg²⁺, indicating apparent first-order approaches to steady state at these Mg²⁺ concentrations. Similarly, adequate fits of eq 1 to the carboxyenzyme data were obtained at 0.24 and 1.0 mM Mg²⁺, indicating apparent first-order approaches to steady state. However, at 10 mM Mg²⁺, the fits of eqs 1 and 2 to the carboxyenzyme and ATP cleavage data, respectively, were poor, and a biphasic process as represented by eq 4 better fitted both sets of data. The fitting of this equation suggests a very small steady-state rate of ATP cleavage at 10 mM Mg²⁺, and separate measurements of this steady-state rate of ATP cleavage support this. Values of the kinetic parameters derived from these fits are shown in Tables 3 and 4. The amplitude of ATP cleavage in the approach to steady state is about 0.8–0.9 mol of P_i/mol of biotin at both 0.24 and 10 mM Mg²⁺, but somewhat lower (0.65 mol of P_i/mol of biotin) at 1 mM Mg²⁺. However, the extent of carboxyenzyme formation is considerably higher at 10 mM Mg²⁺ and more closely matches that of ATP cleavage, whereas at 0.24 and 1.0 mM Mg²⁺, the amplitudes of carboxyenzyme formation are lower than that of ATP cleavage. The apparent first-order rate constant for the approach to steady state of ATP cleavage at 1.0 mM is somewhat lower than that at 0.24 mM Mg²⁺, although the standard error on the estimate of the rate constant at 0.24 mM is quite large (27% of the value). The apparent first-order rate constants for the approach to steady state of carboxyenzyme formation at 0.24 and 1.0 mM Mg²⁺ are the same as and similar in magnitude to those for ATP cleavage. The estimated kinetic parameters for ATP cleavage at 10 mM Mg²⁺ are similar to those for carboxyenzyme formation at 10 mM Mg²⁺. The amplitudes of each phase of the reactions at 10 mM Mg²⁺ are quite well-defined; however, the standard errors on the estimates of the rate constants are large. The estimated steady-state rates of ATP cleavage (turnover number, r) clearly decrease with increasing Mg²⁺ concentrations, the rate at 10 mM Mg²⁺ being effectively zero.

DISCUSSION

It is apparent from the data shown in Figure 1 that dilution of the enzyme from the high concentration of the stock solution in Tris-HCl buffer into the enzyme reactant solution in the absence of acetyl CoA, in preparation for mixing with the ATP reactant solution, resulted in inactivation of the enzyme at 0.1 and 1.0 mM Mg²⁺, but in activation at 10

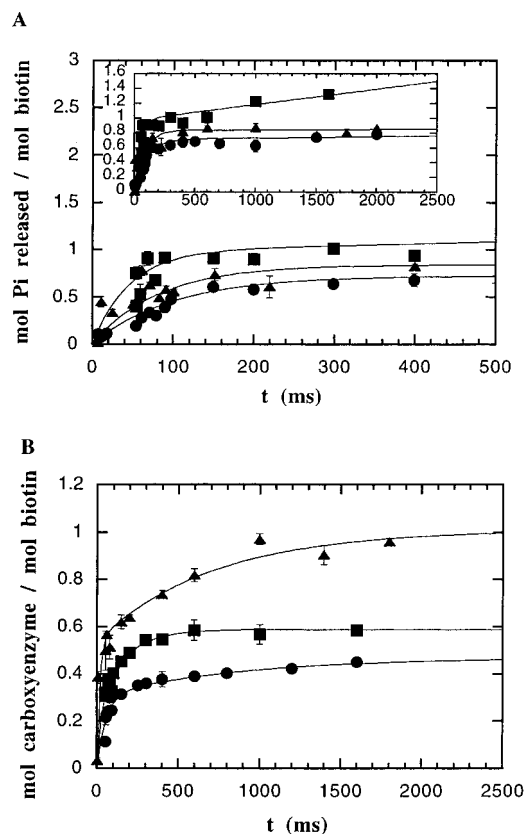


FIGURE 3: Kinetics of ATP cleavage (A) and carboxyenzyme formation (B) measured at 20 °C in 0.1 M Tris-HCl (pH 7.8) in the presence of 0.25 mM acetyl CoA and 0.24 (■), 1.0 (●), and 10 mM free Mg^{2+} (▲), as described in Experimental Procedures. For panel A, 2.5 mM [γ - ^{32}P]ATP and 15 mM $NaHCO_3$ were present, while for panel B, 2.5 mM ATP, 12.5 mM $NaHCO_3$, and 2.5 mM $NaH^{14}CO_3$ were present. In panel A, the amount of P_i released per mole of biotin corresponds to the total number of moles of ATP cleaved per mole of biotin, and the data have been corrected for HCO_3^- -independent ATP cleavage as described in Experimental Procedures. The lines represent nonlinear least-squares fits of eq 2 to the data at 0.24 and 1.0 mM Mg^{2+} and of eq 4 at 10 mM Mg^{2+} . The data points represent the mean and the error bars the standard deviation of three separate measurements from three separate time course experiments. The main panel shows the first 500 ms of the reaction time course, while the inset shows the full time course. In panel B, the number of moles of carboxyenzyme formed per mole of biotin corresponds to the total amount of carboxyl groups that can be transferred to pyruvate on quenching. The lines represent nonlinear least-squares fits of eq 2 to the data at 0.24 and 1 mM Mg^{2+} and of eq 4 at 10 mM Mg^{2+} . In panel B, the data points represent the mean and the error bars the standard deviation derived from three determinations of the radioactivity present as carboxyenzyme at a particular time point. The data as a whole in panel B come from two separate time course experiments.

mM Mg^{2+} . This suggests that there are two opposing processes occurring when the enzyme reactant solution is prepared: (i) an effect of dilution which results in the loss of enzymic activity and (ii) exposure of the enzyme to Mg^{2+} which results in activation of the enzyme. At 0.1 and 1 mM Mg^{2+} , the dilution effect outweighed the activation effect, while the reverse was true at 10 mM Mg^{2+} . It has been known for some time that pyruvate carboxylase from some vertebrate sources was subject to inactivation on dilution (13–15). However, this was originally reported to only occur to a measurable extent below about 4 units/mL (13), and subsequent studies were performed at enzyme concentrations

Table 2: Kinetic Parameters Derived from Fits of Eq 1 or 5 to Carboxyenzyme (CE) Formation Data in the Absence of Acetyl CoA and to Data Simulated from Scheme 1

	k or k_1 (s^{-1})	A or C_A (mol of CE/mol of biotin)	k_2 (s^{-1})
experimental data			
0.24 mM Mg^{2+}	0.013 ± 0.002	0.39 ± 0.02	0.00013 ± 0.00005
1 mM Mg^{2+}	0.020 ± 0.002	0.47 ± 0.01	0.00010 ± 0.00004
10 mM Mg^{2+} ^a	0.030 ± 0.003	0.64 ± 0.01	—
simulated data			
0.24 mM Mg^{2+}	0.014 ± 0.001	0.39 ± 0.02	0.00010 ± 0.00004
1 mM Mg^{2+}	0.018 ± 0.001	0.46 ± 0.01	0.00008 ± 0.00002
10 mM Mg^{2+} ^a	0.027 ± 0.001	0.64 ± 0.003	—

^a Fit of eq 1 to the data.

of below 4 units/mL (14, 15). Both Khew-Goodall et al. (14) and Attwood et al. (15) showed that the phenomenon of dilution inactivation was associated with dissociation of the active tetrameric species of the enzyme into catalytically inactive dimers and monomers. Clearly, from the data presented in the work presented here, it would seem that at least under these conditions, a form of dilution inactivation does occur to a measurable degree at much higher enzyme concentrations than was previously believed to be the case. The increase in the zero time point enzyme specific activities with Mg^{2+} concentration shown in Figure 1 and the observation that, at 10 mM Mg^{2+} , the zero time point activity of the enzyme was higher than that of the stock enzyme suggest that Mg^{2+} activates the enzyme. The overall effect of increasing Mg^{2+} concentration on these zero time point activities may result simply from the activating effect of the ion counterbalancing the loss of activity as a result of dilution of the enzyme to an extent that is dependent on Mg^{2+} concentration. On the other hand, Mg^{2+} may be both protective against dilution inactivation and activatory, both properties being dependent on Mg^{2+} concentration. These effects of Mg^{2+} on dilution inactivation have not been previously reported.

At all Mg^{2+} concentrations, when with the ATP reaction solution was mixed, the enzyme specific activity increased to a level above the 20 units/mg of the stock enzyme solution. These data indicate that MgATP is capable of activating the enzyme. At 0.24 mM Mg^{2+} , the increase in free Mg^{2+} concentration on going from the enzyme solution with only 0.1 mM free Mg^{2+} to the reaction mixture which contains 0.24 mM free Mg^{2+} will also contribute to some extent to this activation effect. At both 0.24 and 1 mM Mg^{2+} , the activation effect may have been achieved by a combination of reversal of dilution inactivation (inducing reassociation of dimers and/or monomers to active tetramers) and increasing the specific activity of already active enzyme or simply by increasing the activity of already active enzyme to an extent that is greater than the activity lost during dilution inactivation. The final level activity of the enzyme that is achieved after mixing with the ATP solution is to some extent dependent on the Mg^{2+} concentration, in that the activity is highest at 10 mM Mg^{2+} . However, there is little difference between final enzyme activities at 0.24 and 1 mM Mg^{2+} , but in both cases, these activities are only about 80% of that at 10 mM Mg^{2+} . This has important implications for the interpretation of the subsequent biotin carboxylation kinetics in the absence of acetyl CoA, in that at 0.24 and 1 mM Mg^{2+}

Table 3: Kinetic Parameters Derived from Fits of Eq 2 to ATP Cleavage Data in the Presence of Acetyl CoA and to Data Simulated from Scheme 1

	k (s^{-1})	A (mol of P_i /mol of biotin)	r (s^{-1})	k' (s^{-1})	A' (mol of P_i /mol of biotin)
experimental data					
0.24 mM Mg^{2+}	21.6 ± 5.9	0.89 ± 0.09	0.280 ± 0.104	—	—
1 mM Mg^{2+}	10.2 ± 1.2	0.65 ± 0.04	0.054 ± 0.033	—	—
10 mM Mg^{2+} ^a	69.5 ± 53.5	0.42 ± 0.18	—	5.5 ± 4.7	0.42 ± 0.17
simulated data					
0.24 mM Mg^{2+}	15.8 ± 0.06	0.968 ± 0.002	0.281 ± 0.002	—	—
1 mM Mg^{2+}	11.4 ± 0.004	0.631 ± 0.0001	0.065 ± 0.0001	—	—
10 mM Mg^{2+} ^a	56.5 ± 0.04	0.536 ± 0.00002	—	1.3 ± 0.003	0.46 ± 0.0002

^a Fit of eq 4 to the data.

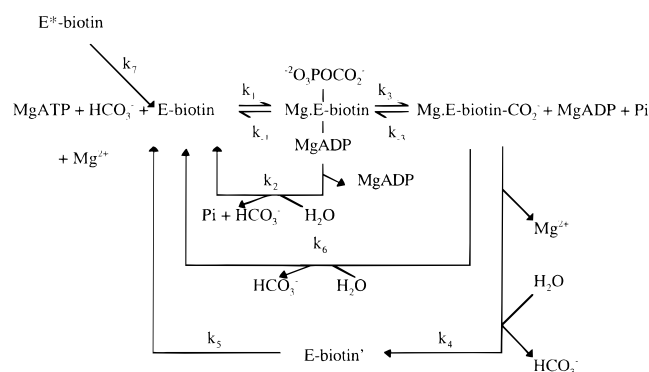
at least, about 20% of the enzyme present appears not to be active.

The fact that the dilution effects described above were not observed in the presence of acetyl CoA is in agreement with previous findings that acetyl CoA prevents dilution inactivation (13, 14). No activation of the enzyme was seen to occur at any Mg^{2+} concentration up to 1 min after mixing the enzyme solution with the ATP solution. This indicates that at least on this short time scale and hence that used to determine the kinetics of the biotin carboxylation reaction in the presence of acetyl CoA (i.e., 2 s), this is not a complicating factor in the interpretation of the kinetics of the biotin carboxylation reaction under these conditions.

The kinetics of both ATP cleavage and carboxyenzyme formation in the absence of acetyl CoA at 10 mM Mg^{2+} are similar to those observed previously at 5 mM Mg^{2+} in that the rate constants for the approach to steady state (see Table 1) are similar to those measured by Legge et al. (7) (0.028 s^{-1} for both carboxyenzyme formation and ATP cleavage). However at 5 mM Mg^{2+} , while the amplitude of the burst phase for carboxyenzyme formation (0.68 ± 0.01 mol/mol of biotin) was similar to that at 10 mM Mg^{2+} (0.64 ± 0.02 mol/mol of biotin; Table 1), that for ATP cleavage was 7.4 ± 0.4 mol of P_i released/mol of biotin at 5 mM Mg^{2+} (7) compared to 1.6 ± 0.1 mol of P_i released/mol of biotin at 10 mM Mg^{2+} (Table 1). For a number of reasons outlined by Legge et al. (7), carboxyenzyme is highly likely to actually represent the enzyme–carboxybiotin complex and not the enzyme–carboxyphosphate complex or the sum of both complexes. Thus below, carboxyenzyme can be regarded as referring to the enzyme–carboxybiotin complex. Legge et al. (7) found that the amplitude of the burst phase of ATP cleavage exceeded 1 mol of P_i released/mol of biotin because of uncoupling between ATP cleavage and carboxyenzyme (enzyme–carboxybiotin complex) formation. Therefore, much of the enzyme–carboxyphosphate complex that formed decomposed without carboxylating biotin, and thus, much of the ATP cleavage required for formation of the enzyme–carboxybiotin complex did not result in formation of the enzyme–carboxybiotin complex. In this work, it would seem that this uncoupling effect is lower at all Mg^{2+} concentrations than that seen by Legge et al. (7) at 5 mM Mg^{2+} since the amplitudes of the burst phase of ATP cleavage are smaller (Table 1). The uncoupling effect would thus appear to increase with increasing Mg^{2+} concentrations up to 5 mM Mg^{2+} , but then decline again at 10 mM Mg^{2+} .

The kinetics of carboxyenzyme formation in the absence of acetyl CoA at 0.24 and 1 mM Mg^{2+} (Figure 2B) are more complex than those at 10 mM Mg^{2+} in that formation of

Scheme 1



carboxyenzyme peaks between about 400 and 600 s, before slowly declining. The model reaction scheme proposed by Legge et al. (7) cannot explain this type of kinetic behavior. In their work, Legge and co-workers focused on the effects of acetyl CoA on the pre-steady-state kinetics of the biotin–carboxybiotin reaction and the Mg^{2+} concentration was fixed at 5 mM. The model reaction scheme that these authors proposed was made as simple as possible to explain their data and did not take into consideration any possible effects of Mg^{2+} concentration. We now propose a new model reaction scheme (Scheme 1), which is a modified version of Scheme 1: reaction 4 from Legge et al. (7) which incorporates the effects of Mg^{2+} concentration and also the activation of the enzyme on mixing with the ATP solution in the absence of acetyl CoA.

In Scheme 1, the activation of the enzyme that occurs on mixing the enzyme solution with the ATP solution is represented by the conversion of E*–biotin (inactive) to E–biotin (active) in a reaction governed by the rate constant k_{+7} . It is assumed that two of the main reacting species, the enzyme–carboxyphosphate complex ($Mg-E-biotin-2O_3POCO_2^- - MgADP$) and the enzyme–carboxybiotin complex ($Mg-E-biotin-CO_2^-$), are enzyme species to which Mg^{2+} is complexed, and the scheme is in accord with the reaction scheme proposed by Warren and Tipton (16) for the overall reaction. Thus, a major area in the reaction scheme where the effects of different Mg^{2+} concentrations manifest themselves on the kinetics of the reaction, lies in the pathway of decarboxylation of the enzyme–carboxybiotin complex. Goodall et al. (17) first showed that increasing the Mg^{2+} concentration was inhibitory with regard to the induction of the decarboxylation of the isolated enzyme–carboxybiotin complex of sheep liver pyruvate carboxylase by analogues of pyruvate. Later, Attwood et al. (18) demonstrated that increasing the Mg^{2+} concentration inhib-

Table 4: Kinetic Parameters Derived from Fits of Eq 1 or 4 to Carboxyenzyme (CE) Formation Data in the Presence of Acetyl CoA and to Data Simulated from Scheme 1

	k (s^{-1})	A (mol of CE/ mol of biotin)	k' (s^{-1})	A' (mol of CE/ mol of biotin)
experimental data				
0.24 mM Mg^{2+}	12.0 ± 1.2	0.56 ± 0.02	—	—
1 mM Mg^{2+}	12.0 ± 1.4	0.40 ± 0.01	—	—
10 mM $Mg^{2+ a}$	98.9 ± 43.4	0.47 ± 0.07	2.1 ± 1.2	0.50 ± 0.08
simulated data				
0.24 mM Mg^{2+}	13.2 ± 0.5	0.56 ± 0.01	—	—
1 mM Mg^{2+}	10.6 ± 0.2	0.41 ± 0.002	—	—
10 mM $Mg^{2+ a}$	56.5 ± 0.007	0.54 ± 0.00002	1.3 ± 0.0003	0.46 ± 0.00003

^a Fit of eq 4 to the data.

ited the carboxylation of pyruvate by the enzyme–carboxybiotin complex and showed that the decarboxylation of the complex in the absence of pyruvate was also inhibited in this manner. In addition, Attwood et al. (18) also showed that the decarboxylation of the enzyme–carboxybiotin complex could occur via two pathways, one in which Mg^{2+} dissociates from the Mg –enzyme–carboxybiotin complex prior to a rapid decarboxylation reaction and one where the Mg^{2+} remains bound during the decarboxylation reaction. Both Goodall et al. (17) and Attwood et al. (18) proposed that the inhibitory action of Mg^{2+} arises because it enhances the binding of the carboxybiotin to the site of the biotin–carboxylation reaction, where it is relatively stable. When the Mg^{2+} dissociates, it allows the movement of the carboxybiotin to the site of the pyruvate carboxylation reaction where it is destabilized and induced to decarboxylate. There is other experimental evidence to indicate that this destabilization occurs, and it has been proposed that the carboxylation of pyruvate may occur via a CO_2 intermediate resulting from decarboxylation of carboxybiotin (10, 19). The process involving Mg^{2+} dissociation is the major route of decarboxylation at low Mg^{2+} concentrations, and as can be seen in Scheme 1, this results in the formation of E –biotin', where the biotin is at the site of the pyruvate carboxylation reaction. To complete the catalytic cycle in this pathway, the biotin must move back to the site of the biotin carboxylation reaction.

At higher Mg^{2+} concentrations, the decarboxylation of the Mg –enzyme–carboxybiotin complex, where Mg^{2+} remains bound, becomes a more important pathway of decarboxylation. The decarboxylation in this pathway presumably occurs at the site of the biotin carboxylation reaction, where, since the carboxybiotin is relatively stable, the reaction is quite slow and not dependent on Mg^{2+} concentration (18). Thus, the flux through each pathway in Scheme 1 will be dependent on the Mg^{2+} concentration, as will the accumulation of enzyme in the E –biotin' form.

As described by Legge et al. (7), to model the reactions as simply as possible using Scheme 1, the values of the reverse rate constants k_{-1} and k_{-4} were fixed at zero. The values of k_7 were fixed at the estimated first-order rate constants derived for the activation of the enzyme from the data shown in Figure 1. The value of k_6 was fixed at $0.00025 s^{-1}$ which was approximated from the value experimentally determined at $0^\circ C$ (18), assuming a Q_{10} of 2. From Figure 1, it is apparent that the final overall enzyme activity is dependent on Mg^{2+} concentration. In modeling Scheme 1, we assumed that the enzyme was fully active at 10 mM Mg^{2+}

(additional experiments showed that further increasing the Mg^{2+} concentration to 20 mM did not result in increased enzyme specific activity, data not shown). Thus, at 10 mM Mg^{2+} , the maximum enzyme activity was set at 1 mol/mol of biotin, while at 0.24 and 1.0 mM Mg^{2+} , the maximum enzyme activity was set at 0.8 mol/mol of biotin. Initial values of the proportion of enzyme in the E^* –biotin form were fixed using the values obtained from the data in Figure 1. Thus, at 10 mM Mg^{2+} , at time zero, $[E$ –biotin] + $[E$ –biotin'] + $[E^*$ –biotin] = 1 mol/mol of biotin, while at 0.24 and 1 mM Mg^{2+} , the same sum of enzyme species present at zero time is 0.8 mol/mol of biotin. In the presence of acetyl CoA, the sum of enzyme species present at zero time at all Mg^{2+} concentrations was assumed to be 1 mol/mol of biotin, with no enzyme present as E^* –biotin. Finally, a simple form of Scheme 1 is one where the rate-limiting step in the interconversion of E –biotin to Mg – E –biotin– $O_2COPO_3^{2-}$ – $MgADP$ is the actual cleavage of ATP in the Mg – ATP – HCO_3^- – Mg – E –biotin complex. In this case, the substrates and Mg^{2+} bind very rapidly to the enzyme and k_1 represents a true first-order catalytic step in the reaction that does not vary with Mg^{2+} concentration. In the more general case in Scheme 1, k_1 represents the rate-limiting step in the formation of the enzyme–carboxyphosphate complex (Mg – E –biotin– $O_2COPO_3^{2-}$ – $MgADP$), and this may be the true first-order ATP cleavage step or may represent a substrate or Mg^{2+} binding step which is pseudo-first-order since the concentrations of substrates and Mg^{2+} are much higher than that of the enzyme. Simulations of Scheme 1 were performed; eq 2 was fitted to the simulated data for ATP cleavage, while to the simulated data for the formation of Mg – E –biotin– CO_2^- were fitted eq 1 for the 10 mM Mg^{2+} data and eq 5 for the 0.24 and 1 mM Mg^{2+} data. Values of the rate constants, other than k_6 and k_7 , were varied, as were zero time values of the proportion of the enzyme in the E –biotin form. This process was continued until the estimates of the parameters obtained by fitting eq 1, 2, or 5, as appropriate, to the simulated data fell within the range of the standard errors of the parameter estimates obtained from the fits of the equations to the experimental data (see Tables 1 and 2), and the simulation was thus deemed “adequate”. The process also involved searches for sets of parameters that gave simulations to fit the experimental data, in which the value of k_1 was the same at all Mg^{2+} concentrations. It should be emphasized that the sets of values of the kinetic parameters presented in Table 5 do not represent unique solutions in fitting Scheme 1 to the data. In the following discussion, there is a description of how

Table 5: Parameter Values Used in the Simulations of Scheme 1 for the Reactions in the Presence or Absence of Acetyl CoA^a

[Mg ²⁺] (mM)	<i>k</i> ₁	<i>k</i> ₂	<i>k</i> ₃	<i>k</i> ₄	<i>k</i> ₅	<i>k</i> ₆	<i>k</i> ₇	E-b ₀ ^b	E*-b ₀ ^b
absence of acetyl CoA									
0.24	0.09	1.29	1.00	0.0025	0.0020	0.00025	0.022	0.004	0.38
1.0	0.09	2.83	1.00	0.0028	0.0036	0.00025	0.023	0.280	0.24
10.0	0.09	1.53	1.00	0.0017	0.0031	0.00025	0.021	0.470	0.21
presence of acetyl CoA									
0.24	31.4	940	1000	0.100	0.350	0.00025	—	0.50	—
1.0	18.5	620	1000	0.050	0.069	0.00025	—	0.39	—
10.0	56.6	0	1000	0.000	1.290	0.00025	—	0.55	—

^a All values of rate constants have units of s⁻¹. ^b E-b₀ (E-biotin₀) and E*-b₀ (E*-biotin₀) are the amounts of these enzyme species present at time zero, expressed as proportions of total active and activatable enzyme and have units of moles of enzyme species per mole of biotin.

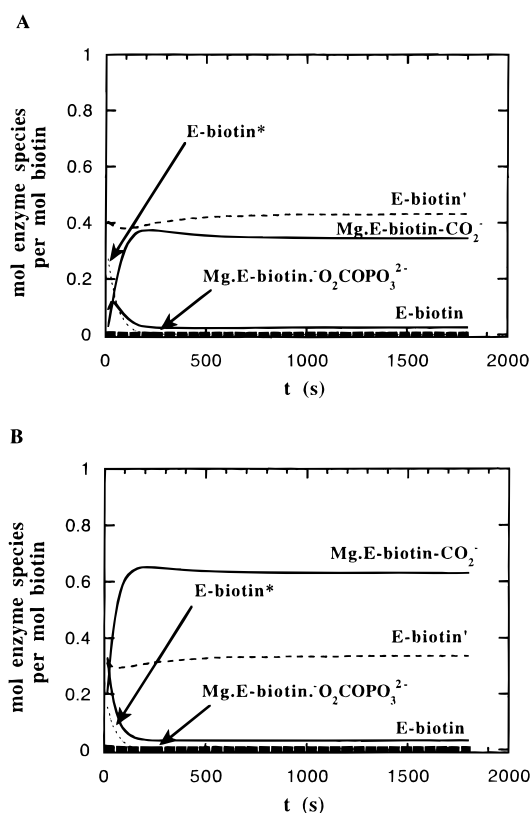


FIGURE 4: Data simulated from Scheme 1 (in the absence of acetyl CoA) using the kinetic parameters shown in Table 5, at 0.24 (A) and 10 mM Mg²⁺ (B).

some parameter values could be varied and the simulations still be regarded as “adequate” with respect to fits of the various equations (eqs 1, 2, 4, and 5) to the simulated data.

Figure 4 shows simulations of changes in all of the enzyme species in the approach to steady state at 0.24 (A) and 10 mM Mg²⁺ (B). At both Mg²⁺ concentrations, there is little accumulation of the enzyme-carboxyphosphate complex during the course of the experiment, and in the steady state, there is little enzyme present in the E-biotin form. The low proportion of enzyme present in the steady state in the form of the enzyme-carboxyphosphate complex and E-biotin agrees with the modeling by Legge et al. (7), using the simpler form of Scheme 1. At both Mg²⁺ concentrations, the major species present at steady state are the enzyme-carboxybiotin complex and E-biotin'. The effect of increasing Mg²⁺ concentrations is to change this distribution so that at low Mg²⁺ concentrations, there is more enzyme present as E-biotin' than as the enzyme-carboxybiotin complex, whereas at high Mg²⁺ concentrations, the situation is

reversed. The inclusion of the E-biotin' enzyme species in the model reaction scheme explains the discrepancy between the steady-state level of the enzyme-carboxybiotin complex and the total enzyme level present that Legge et al. (7) observed in their experiments, but found difficult to explain on the basis of their proposed model reaction scheme.

From Table 5, it is apparent that the “active” enzyme present at zero time is distributed between E-biotin and E-biotin', suggesting an equilibrium exists between the two enzyme species prior to the start of the reaction. It was possible to obtain a simulation in which all of the active enzyme was in the E-biotin form at zero time by varying *k*₂/*k*₃, *k*₄, and *k*₅, which also fitted the experimental data well, but only at 1 mM Mg²⁺. At the other two Mg²⁺ concentrations, in similar simulations, the rate and initial amplitude of formation of the enzyme-carboxybiotin complex were too large to fit the experimental data. According to the simulations represented by the figures shown in Table 5, as the Mg²⁺ concentration increased, the proportion of enzyme in the E-biotin form also increased. This indicates that the putative equilibrium between E-biotin and E-biotin' is dependent on the Mg²⁺ concentration. Some variation in the amounts of E-biotin₀ still produced simulations which when eq 1, 2, or 5 was fitted as appropriate, gave estimated parameters that lay within the standard errors of those shown in Tables 1 and 2. Thus, for 0.24, 1, and 10 mM Mg²⁺, the acceptable values for E-biotin₀ were 0–0.01, 0.26–0.28, and 0.47–0.51, respectively. Thus, even with these ranges of possible values of E-biotin₀, the general pattern of increasing proportions of the enzyme present as E-biotin at zero time with increasing Mg²⁺ concentrations is maintained.

In the presence of acetyl CoA, Legge et al. (7) were unable to model the biotin carboxylation reaction using the same form of the reaction scheme that they used to model the reaction in the absence of acetyl CoA. They were obliged to invoke the existence of an equilibrium between the enzyme-carboxyphosphate complex and the enzyme-carboxybiotin complex. However, the reaction scheme that Legge and co-workers used did not include the enzyme form, E-biotin'. In the work presented here, apart from the lack of inactive enzyme (E*-biotin) present at zero time, we have found that the unmodified form of Scheme 1 could be used to model the biotin carboxylation reaction in the presence of acetyl CoA.

As with the reaction in the absence of acetyl CoA, simulations were performed, and at 0.24 and 1 mM Mg²⁺, eq 2 was then fitted to the simulated ATP cleavage data; in this case, however, eq 1 was fitted to the simulated

carboxyenzyme formation data. At 10 mM Mg^{2+} , eq 4 was fitted to both the simulated ATP cleavage and carboxyenzyme formation data. A simulation was deemed “adequate” if all of the estimates of the kinetic parameters obtained from the fits to both the ATP cleavage and carboxyenzyme formation data for a particular simulation fell within the standard errors of the values derived from fits to the experimental data. The value of k_6 was fixed at the value used in the simulations in the absence of acetyl CoA as there is no evidence that this rate constant is affected by acetyl CoA. The values of the kinetic parameters shown in Table 5 for the reaction in the presence of acetyl CoA are the values of parameters used to obtain the simulations from which the fits shown in Tables 2 and 3 were derived.

No “adequate” simulations were found where all of the enzyme was present as E-biotin at zero time; thus, again it would seem that an equilibrium existed between E-biotin and E-biotin' prior to starting the reaction. In this case, however, there was no very marked dependence on Mg^{2+} concentration of the distribution of enzyme between the two species, with the values for E-biotin₀ at 0.24, 1.0, and 10 mM Mg^{2+} being 0.48–0.50, 0.385–0.395, and 0.43–0.55 mol/mol, respectively.

Unlike the simulations for the reaction in the absence of acetyl CoA, it was not possible to obtain “adequate” simulations for the reaction in the presence of acetyl CoA in which the value of k_1 was constant at all Mg^{2+} concentrations. This suggests that in the presence of acetyl CoA, the reaction represented by k_1 is not simply one where the rate-limiting step in the interconversion of E-biotin to Mg-E-biotin- $\text{O}_2\text{COPO}_3^{2-}$ is the actual cleavage of ATP in the Mg-ATP- HCO_3^- -Mg-E-biotin complex. In the presence of acetyl CoA, the rate-limiting step in this reaction must change with changing Mg^{2+} concentrations and may include Mg^{2+} binding or substrate binding steps. The values of the ratio of k_1 for which “adequate” simulations could be obtained at 0.24, 1.0, and 10 mM Mg^{2+} were 31.2–31.4, 18.5–18.8, and 56–123 s^{-1} , respectively.

Figure 5 shows simulations of all enzyme species using the parameter values shown in Table 5 at 0.24 (A) and 10 mM Mg^{2+} (B) in the presence of acetyl CoA. At all Mg^{2+} concentrations, there is no appreciable accumulation of the enzyme-carboxyphosphate complex during any part of the reaction and the steady-state levels of E-biotin are all zero. In the steady state, enzyme is present as a mixture of the enzyme-carboxybiotin complex or E-biotin'. At all Mg^{2+} concentrations, the proportion of enzyme present as E-biotin' declines in the approach to steady state. The simulations suggest that steady state has only been substantially achieved at 10 mM Mg^{2+} over the time courses of the experiments. At 0.24 mM Mg^{2+} , steady state is achieved only after about 10–20 s, with final steady-state levels of the enzyme-carboxybiotin complex and E-biotin' of 0.78 and 0.22 mol/mol of biotin, respectively. At 1 mM Mg^{2+} , steady state is achieved only after 20–30 s, with final levels of the enzyme-carboxybiotin complex and E-biotin' of 0.58 and 0.42 mol/mol of biotin, respectively. Thus, in fact, in simulations at all Mg^{2+} concentrations, formation of the enzyme-carboxybiotin complex is a biphasic process in the approach to steady state, with rapid conversion of E-biotin to enzyme-carboxybiotin, governed largely by k_1 , being followed by a slower conversion of E-biotin' governed in

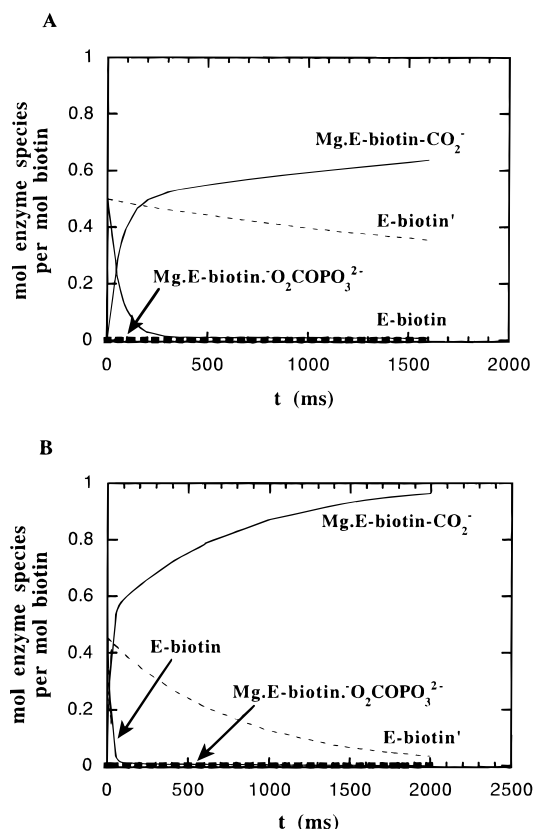


FIGURE 5: Data simulated from Scheme 1 (in the presence of acetyl CoA) using the kinetic parameters shown in Table 5, at 0.24 (A) and 10 mM Mg^{2+} (B).

part by k_5 . In fact, it was possible to obtain fits of eq 4 to the carboxyenzyme formation data at both 0.24 and 1.0 mM Mg^{2+} . The rate constants estimated from these fits were as follows: $k = 22 \pm 3 \text{ s}^{-1}$ and $k' = 4.3 \pm 1.5 \text{ s}^{-1}$ at 0.24 mM Mg^{2+} and $k = 18 \pm 2 \text{ s}^{-1}$ and $k' = 1.1 \pm 0.5 \text{ s}^{-1}$ at 1.0 mM Mg^{2+} . This also means that the apparent steady-state rate of ATP cleavage observed experimentally at 0.24 and 1.0 mM is not truly linear, but slightly curved owing to the net conversion of E-biotin' to the enzyme-carboxybiotin complex in the approach to steady state. At these Mg^{2+} concentrations, there is still appreciable turnover in the catalytic cycle; thus, the net conversion of E-biotin' to the enzyme-carboxybiotin complex makes a contribution to the overall apparent steady-state rate. At 10 mM Mg^{2+} , however, there is very little turnover in the catalytic cycle, and thus, ATP cleavage becomes more obviously a biexponential process, with the rate of the slow phase being determined by k_5 . At 10 mM Mg^{2+} , virtually all of the enzyme accumulates in the form of the enzyme-carboxybiotin complex at steady state.

When k_2 and k_3 were equal to or greater than 10 times the value of k_1 , the absolute values of the individual rate constants did not affect the simulation as long as the ratio k_2/k_3 was that of the rate constants shown in Table 5 (under these circumstances, formation of the enzyme-carboxyphosphate complex is rate-limiting in the formation of the enzyme-carboxybiotin complex). However, the value of the ratio of k_2/k_3 did affect the simulations. Similar effects of the values of k_2 and k_3 on model simulations were noted by Legge et al. (7), and thus, Scheme 1 still retains the characteristics of the original reaction scheme, in that k_2/k_3

determines the degree of coupling of ATP cleavage to enzyme carboxybiotin formation, with k_1 being smaller than k_2 and k_3 . As with E-biotin₀ values, fits of Scheme 1 to the data were obtained with different absolute values of k_2/k_3 ; for example, fits to the 0.24, 1, and 10 mM Mg²⁺ experimental data were obtained with ranges of k_2/k_3 ratios of 1.2–1.3, 2.7–2.9, and 1.40–1.50, respectively, in the absence of acetyl CoA and 0.94–0.96, 0.61–0.62, and 0–0.01, respectively, in its presence. Thus, from Table 5, it can be seen that as the Mg²⁺ concentration increases from 0.24 to 10 mM in the presence of acetyl CoA, the ratio k_2/k_3 decreases markedly to close to zero at 10 mM Mg²⁺. In the absence of acetyl CoA, however, k_2/k_3 initially increases by a factor of 2.2 but then declines at 10 mM Mg²⁺, to a value that is a little higher than that at 0.24 mM Mg²⁺. If we assume that Mg²⁺ remains bound to the enzyme during the conversion of the enzyme–carboxyphosphate complex to the enzyme–carboxybiotin complex, this would indicate that Mg²⁺ concentration has its effect on k_2/k_3 by changing the value of k_2 . This would suggest that the abortive decarboxylation of the carboxyphosphate and conversion of the enzyme–carboxyphosphate complex back to E-biotin involves the dissociation and rebinding of Mg²⁺ to the enzyme. In the presence of acetyl CoA, the Mg²⁺ dissociation step may be rate-limiting at all Mg²⁺ concentrations, and the rate constant for the step decreases with increasing Mg²⁺ concentrations. Thus, the ratio of k_2/k_3 clearly shows a marked dependency on Mg²⁺ concentration, with the value of the ratio decreasing with increasing Mg²⁺ concentrations. This indicates that increasing the Mg²⁺ concentration enhances the coupling between ATP cleavage and formation of the enzyme–carboxybiotin complex. In the absence of acetyl CoA, the rate-limiting step depends on Mg²⁺ concentration. Thus, at 0.24 mM Mg²⁺, the Mg²⁺-rebinding step may be rate-limiting, while at 10 mM Mg²⁺, the dissociation step may be rate-limiting. At intermediate Mg²⁺ concentrations, an optimal rate of reaction would be achieved, possibly at 5 mM Mg²⁺, corresponding to that observed by Legge et al. (7).

“Adequate” fits to the data at 0.24, 1, and 10 mM Mg²⁺ were obtained with k_4 values of 0.0024–0.0025, 0.0025–0.0028, and 0.0016–0.0017 s^{−1}, respectively, in the absence of acetyl CoA and 0.03–0.10, 0.05–0.12, and 0–0.06 s^{−1}, respectively, in its presence. Because of the overlap between the k_4 values between 0.24 and 1.0 mM Mg²⁺, the effect of Mg²⁺ on k_4 at these concentrations is not clear; however, there may be a decrease in k_4 between 1.0 and 10 mM Mg²⁺. In their studies on the rate of decarboxylation of the isolated enzyme–carboxybiotin complex at 0 °C, Attwood et al. (18) found that the observed rate constant for the process (equivalent to k_4) at 1 mM Mg²⁺ was about 67% of that at 0.24 mM Mg²⁺, while that at 10 mM Mg²⁺ was 14% of that at 0.24 mM Mg²⁺. We cannot directly compare the values from Attwood et al. (18) with the current values because of the difference in temperature at which the experiments were performed and the presence of MgATP and HCO₃[−] in the current experiments. However, the figures described above suggest that there is a larger effect on k_4 in going from 1.0 to 10 mM Mg²⁺ than in going from 0.24 to 1.0 mM Mg²⁺.

“Adequate” fits to the data at 0.24, 1, and 10 mM Mg²⁺ were obtained with ranges of k_5 values of 0.0018–0.0022, 0.0034–0.0038, and 0.0028–0.0032 s^{−1}, respectively, in the

absence of acetyl CoA and 0.35–0.38, 0.03–0.07, and 0.9–3.3 s^{−1}, respectively, in its presence. Thus, again the general pattern of the variation of k_5 with Mg²⁺ concentration seen in Table 5 is retained. The fact that k_5 does not simply increase with increasing Mg²⁺ concentrations suggests that the rate-limiting step in this reaction in Scheme 1 is not simply the binding of Mg²⁺ to E-biotin'. The reaction also involves the movement of biotin from the site of the decarboxylation of the carboxybiotin (the pyruvate carboxylation site) to the site of the biotin carboxylation reaction. This reaction may also contain some substrate binding steps. It would appear that as the Mg²⁺ concentration increases, the rate-limiting step in the reaction changes.

Measurements of the turnover numbers for the full pyruvate carboxylation reaction were taken in the absence of acetyl CoA, at the three different Mg²⁺ concentrations, using the spectrophotometric assay similar to that described in Experimental Procedures, but under conditions similar to those used to measure the biotin carboxylation reaction and with 20 mM pyruvate present in the reaction mixture. The turnover numbers measured at 0.24, 1.0, and 10 mM Mg²⁺ were 0.0020 ± 0.0004, 0.0024 ± 0.0007, and 0.0049 ± 0.0010 s^{−1}, respectively (the figures are the means and standard deviations of three measurements). Generally speaking, these values are similar to the values of k_5 described above and suggest that the rate-limiting step in the pyruvate carboxylation reaction may be that represented by this rate constant, possibly corresponding to the return of biotin to the site of the biotin carboxylation reaction.

Measurements of the turnover numbers of the full pyruvate carboxylation reaction in the presence of acetyl CoA were performed as described above and gave values at 0.24, 1.0, and 10 mM Mg²⁺ of 6.4 ± 0.5, 10.3 ± 0.1, and 11.8 ± 0.7 s^{−1}, respectively. Although these values are on the same order of magnitude as the values of k_1 in Table 5, they are all consistently lower. If the proposed reaction scheme is correct for the reaction in the presence of acetyl CoA, it seems unlikely that k_1 represents the rate-limiting step in the catalytic cycle. However, there is a possibility that the presence of pyruvate may reduce the rate of the reaction represented by k_1 , since Attwood and Graneri (20) noted that the pyruvate analogue, oxamate, inhibited phosphate transfer between carbamoyl phosphate and ADP.

From the work of Attwood et al. (18), it is clear that the decarboxylation of the isolated enzyme–carboxybiotin complex is much more rapid in the presence of pyruvate than in its absence (by a factor of about 80 000 at 0 °C at 10 mM Mg²⁺). If this remains the case at 20 °C, under the current reaction conditions, this would give rise to very large values of k_4 in the presence of pyruvate, thus making it unlikely that this step is rate-limiting in the catalytic cycle, except perhaps at 10 mM Mg²⁺. This leaves the step represented by k_5 as a candidate for the rate-limiting step in the catalytic cycle of the full pyruvate carboxylation reaction, at least at 0.24 and 1.0 mM Mg²⁺. The values of this rate constant in the absence of pyruvate are all much too small to correspond to the measured turnover numbers of the full pyruvate carboxylation reaction. This indicates that in the presence of pyruvate, either the rate of this reaction step is enhanced or the reaction proceeds via a mechanism in which Mg²⁺ dissociation does not occur and hence this reaction step is bypassed. McClure et al. (21) suggested that pyruvate binding

may enhance the binding of bicarbonate which is indicative of a positive interaction between the sites of reaction II and that of reaction I. Thus, it is possible that pyruvate enhances the rate of a rate-limiting step in the reaction represented by k_5 . It is clear from the results Attwood et al. (18) that carboxylation of pyruvate by the isolated enzyme-carboxybiotin complex at 0 °C is dependent on Mg^{2+} concentration. However, Warren and Tipton (16) found kinetic evidence to support a reaction scheme for the full pyruvate carboxylation reaction at 30 °C in the presence of acetyl CoA in which pyruvate carboxylation by the enzyme-carboxybiotin complex is not dependent on Mg^{2+} concentration, with the Mg^{2+} remaining bound during the whole catalytic cycle. If this were the case under our reaction conditions, then in the presence of pyruvate, k_4 and k_5 in Scheme 1 could be replaced by a single rate constant which represented a rate-limiting step in a reaction which covered both carboxylation of pyruvate and movement of biotin back to the site of reaction (I). This rate constant could also then represent the rate-limiting step in the whole catalytic cycle.

In summary, Scheme 1 can represent the experimental data both in the presence and in the absence of acetyl CoA. The accumulation in the steady state of the enzyme in the form of E-biotin' explains the discrepancy between the total amount of enzyme present and that accumulated in the form of the enzyme-carboxybiotin complex. In addition, the model predicts that prior to the start of the reaction there is an equilibrium between E-biotin and E-biotin' which is strongly dependent on Mg^{2+} concentration in the absence of acetyl CoA. In both the presence and absence of acetyl CoA, the model predicts that there will be virtually no accumulation of the enzyme-carboxyphosphate complex, and this may explain the lack of success in trapping this putative intermediate in reactions catalyzed by biotin-dependent enzymes (22, 23). In the absence of acetyl CoA, Scheme 1 can be modeled where k_1 is independent of Mg^{2+} concentration; however, this is not the case in the presence of acetyl CoA. In both the presence and absence of acetyl CoA, the coupling between ATP cleavage and the formation of the enzyme-carboxybiotin complex is predicted to be dependent on Mg^{2+} concentration. This effect would appear to be brought about by the action of Mg^{2+} on the rate of abortive decarboxylation of the enzyme-carboxyphosphate complex, and in the presence of acetyl CoA, increasing the Mg^{2+} concentration results in a decrease in the rate of this process.

APPENDIX

(a) *Without Acetyl CoA*. The differential equations that were used in the simulations of Scheme 1 were as follows:

$$\begin{aligned} [\text{E-biotin}]' &= k_2[\text{Mg-E-biotin}-^{-2}\text{O}_3\text{POCO}_2^{-}-\text{MgADP}] + k_5[\text{E-biotin}'] + k_6[\text{Mg-E-biotin-CO}_2^{-}] + k_7[\text{E*}-\text{biotin}] - k_1[\text{E-biotin}] \\ [\text{Mg-E-biotin}-^{-2}\text{O}_3\text{POCO}_2^{-}-\text{MgADP}]' &= k_1[\text{E-biotin}] - (k_2 + k_3)[\text{Mg-E-biotin}-^{-2}\text{O}_3\text{POCO}_2^{-}-\text{MgADP}] \end{aligned}$$

$$\begin{aligned} [\text{Mg-E-biotin-CO}_2^{-}]' &= k_3[\text{Mg-E-biotin}-^{-2}\text{O}_3\text{POCO}_2^{-}-\text{MgADP}] - (k_4 + k_6)[\text{Mg-E-biotin-CO}_2^{-}] \end{aligned}$$

$$[\text{E-biotin}]' = k_4[\text{Mg-E-biotin-CO}_2^{-}] - k_5[\text{E-biotin}']$$

$$[\text{E*}-\text{biotin}]' = -k_7[\text{E*}-\text{biotin}]$$

$$[\text{P}_i \text{ cleaved from ATP}]' = k_1[\text{E-biotin}]$$

The rate of cleavage of P_i from ATP can be expressed in the last equation since the reaction step governed by k_1 is the step in which the γ -phosphate is cleaved from ATP. The reaction is quenched in HCl and the mixture treated with trichloroacetic acid; the enzyme is thus denatured, and since carboxyphosphate is a very labile intermediate, this intermediate is almost certainly completely hydrolyzed, liberating P_i . Thus, the measured amount of P_i includes that from carboxyphosphate, any enzyme-bound P_i , and free P_i and so truly represents the amount of P_i cleaved from ATP. All concentrations are expressed as moles per mole of active enzyme present at the end of the reaction (see Discussion).

(b) *With Acetyl CoA*. The differential equations are the same as those used when acetyl CoA was absent except that the term $[\text{E*}-\text{biotin}]$ is absent from all equations and the concentrations are all expressed as moles per mole of biotin, since all of the enzyme is active from the outset of the reaction in the presence of acetyl CoA (see Discussion).

REFERENCES

- Attwood, P. V. (1995) *Int. J. Biochem. Cell Biol.* 27, 231–249.
- Knowles, J. R. (1989) *Annu. Rev. Biochem.* 58, 195–221.
- Scrutton, M. C., Keech, D. B., and Utter, M. F. (1965) *J. Biol. Chem.* 240, 574–581.
- Phillips, N. F. B., Snoswell, M. A., Chapman-Smith, A., Keech, D. B., and Wallace, J. C. (1992) *Biochemistry* 31, 9445–9450.
- Attwood, P. V. (1993) *Biochemistry* 32, 12736–12742.
- Attwood, P. V., and Graneri, B. D. L. A. (1992) *Biochem. J.* 287, 1011–1017.
- Legge, G. B., Branson, J. P., and Attwood, P. V. (1996) *Biochemistry* 35, 3849–3856.
- Goss, N. H., Dyer, P. Y., Keech, D. B., and Wallace, J. C. (1979) *J. Biol. Chem.* 254, 1734–1739.
- Helmerhorst, E., and Stokes, G. B. (1980) *Anal. Biochem.* 104, 130–135.
- Attwood, P. V., and Cleland, W. W. (1986) *Biochemistry* 25, 8191–8196.
- Rylatt, D. B., Keech, D. B., and Wallace, J. C. (1977) *Arch. Biochem. Biophys.* 183, 113–122.
- Morrison, J. F. (1979) *Methods Enzymol.* 63, 257–294.
- Ashman, L. K., Keech, D. B., Wallace, J. C., and Nielsen, J. (1972) *J. Biol. Chem.* 247, 5818–5824.
- Khew-Goodall, Y. S., Johannssen, W., Attwood, P. V., Wallace, J. C., and Keech, D. B. (1991) *Arch. Biochem. Biophys.* 284, 98–105.
- Attwood, P. V., Johannssen, W. M., Chapman-Smith, A., and Wallace, J. C. (1993) *Biochem. J.* 290, 583–590.
- Warren, G. B., and Tipton, K. F. (1974) *Biochem. J.* 139, 311–320.
- Goodall, G. J., Baldwin, G. S., Wallace, J. C., and Keech, D. B. (1981) *Biochem. J.* 199, 603–609.

18. Attwood, P. V., Wallace, J. C., and Keech, D. B. (1984) *Biochem. J.* 219, 243–251.
19. Attwood, P. V., Tipton, P. A., and Cleland, W. W. (1986) *Biochemistry* 25, 8197–8205.
20. Attwood, P. V., and Graneri, B. D. L. A. (1991) *Biochem. J.* 273, 443–448.
21. McClure, W. R., Lardy, H. A., Wagner, M., and Cleland, W. W. (1971) *J. Biol. Chem.* 246, 3569–3578.
22. Wallace, J. C., Phillips, N. F. B., Snoswell, M. A., Goodall, G. J., Attwood, P. V., and Keech, D. B. (1985) *Ann. N.Y. Acad. Sci.* 447, 169–188.
23. Ogita, T., and Knowles, J. R. (1988) *Biochemistry* 27, 8028–8033.

BI992825V